



Constructing processing map of Ti40 alloy using artificial neural network

SUN Yu¹, ZENG Wei-dong¹, ZHAO Yong-qing²,
ZHANG Xue-min¹, MA Xiong¹, HAN Yuan-fei¹

1. State Key Laboratory of Solidification Processing, School of Materials Science and Engineering, Northwestern Polytechnical University, Xi'an 710072, China;
2. Northwest Institute for Nonferrous Metal Research, Xi'an 710016, China

Received 17 June 2010; accepted 15 August 2010

Abstract: Based on the experimental data of Ti40 alloy obtained from Gleeble-1500 thermal simulator, an artificial neural network model of high temperature flow stress as a function of strain, strain rate and temperature was established. In the network model, the input parameters of the model are strain, logarithm strain rate and temperature while flow stress is the output parameter. Multilayer perceptron (MLP) architecture with back-propagation algorithm is utilized. The present study achieves a good performance of the artificial neural network (ANN) model, and the predicted results are in agreement with experimental values. A processing map of Ti40 alloy is obtained with the flow stress predicted by the trained neural network model. The processing map developed by ANN model can efficiently track dynamic recrystallization and flow localization regions of Ti40 alloy during deforming. Subsequently, the safe and instable domains of hot working of Ti40 alloy are identified and validated through microstructural investigations.

Key words: Ti40 alloy; processing map; artificial neural network

1 Introduction

Titanium alloys have been increasingly and extensively applied in the field of aerospace because of their excellent combination of high specific strength (strength-to-weight ratio) which is maintained at elevated temperature, fracture resistant characteristics and exceptional resistance to corrosion[1]. Because the advanced engines need to have good mechanical properties and burn resistance for some crucial parts, much more attention has been paid to burn-resistant titanium alloys in different countries, especially on Ti-V-Cr burn-resistant titanium alloys. In the past few years, Alloy C (Ti-35V-15Cr) from USA and Ti-25V-15Cr-2Al-0.2C from UK have been developed and applied in engines successfully by Pratt, Whitney and IRC respectively[2–3]. Ti40 (Ti-25V-15Cr-0.2Si) alloy, a stable β type burn-resistant titanium alloy, was developed by Northwest Institute for Nonferrous Metal Research of China in 1996[4]. The researchers have systemically and deeply studied its burn-resistant mechanism[5], hot workability and microstructure

evolution[6], fracture criterion[7], and mechanical properties [8]. Although Ti40 alloy possesses better mechanical properties and burn resistance than other burn-resistant titanium alloys, but it has poor workability and its properties are still difficultly controlled during hot work processing because of its edge cracking. Therefore, it is necessary to properly understand the constitutive flow behavior of this alloy under processing conditions.

Recently, “systems approach” philosophy[9] has been introduced using science-based methodology such as dynamic materials model (DMM) to develop a processing map to optimize the workability and control the microstructure. Briefly, a processing map is generated using data of flow stress as a function of temperature and strain rate over a wide range. The flow stress variation with strain rate at a given temperature is curve fitted using a spline function and the strain rate sensitivity is calculated as a function of strain rate. The processing map identifies “safe” and “unsafe” domains for processing of materials. The various mechanisms in the “unsafe” domain are manifested as flow localization, adiabatic shear band formation and dynamic strain ageing which are not helpful to the processing of the

Foundation item: Project(2007CB613807) supported by the National Basic Research Program of China; Project(NCET-07-0696) supported by the New Century Excellent Talents in University, China; Project(35-TP-2009) supported by the Fund of the State Key Laboratory of Solidification Processing in Northwestern Polytechnical University, China

Corresponding author: SUN Yu; Tel/Fax: +86-29-88494298; E-mail: sunyu.npu@gmail.com

DOI: 10.1016/S1003-6326(11)60693-6

material and also result in poor mechanical properties of the product. The processing map has become a powerful tool to design and optimize hot deformation processes. It not only describes the microstructural evolution mechanism and the flow instability domains under certain conditions but also provides a optimum deformation temperature range and strain rate range. As a result, it has been widely applied to many kinds of alloys such as aluminium alloys[10], stainless steels[11], Ni-based alloys[12] and titanium alloys[13–14].

Conventionally, the processing maps are constructed by means of curve fitting technique. However, the affecting factors (strain, strain rate and temperature) of flow stress presents highly complicated non-linear and interaction relationship during hot deformation, which leads to the fact that strain rate values of hot compression tests cover a range of four to five orders of magnitude. Thus it cannot be appropriate to obtain processing maps using curve fitting technique and interpolation to compute the flow stress values at proper temperature and strain rate intervals. With the development of artificial intelligence, researchers have paid a great deal of attention to the solution of non-linear and interaction problems in hot deformation behavior of metal alloys[15–18]. One of the main advantages of artificial neural network is that it is not necessary to postulate a mathematical model at first or identify its parameters. It has been successfully applied in many areas of engineering and has produced promising preliminary results in the fields of material modeling and processing[19–21]. However, the application of artificial neural network to construct processing map for titanium alloys is scarce. Hence, in the present investigation, artificial neural network model was developed to predict the flow stress of Ti40 alloy under different deformation conditions. Based on the trained artificial neural network (ANN), the processing map of Ti40 alloy was obtained and verified by metallographical observation.

2 Experimental

A 40 kg Ti40 alloy ingot with a diameter of 140 mm was used in this investigation. Its nominal chemical composition is Ti-25V-15Cr-0.2Si. The testing specimens of Ti40 alloy from the cast ingot were machined into cylinder with 8 mm in diameter and 12 mm in length, and the cylinder ends were grooved for retention of the glass lubricants. The hot compression tests were carried out on Gleeble–1500 thermo-simulation machine in the temperature range of 900–1100 °C with 50 °C interval and strain rates of 0.01, 0.1, 1 and 10 s⁻¹. The high reduction of the specimens was 50%. All the specimens were cooled in the air in order to avoid cracking. The deformed specimens for

microstructural analysis were sectioned and prepared by the standard metallographic procedure. Microstructure observations were carried out on Olympus/PMG3 optical microscope.

3 Theory of processing map based on DMM

On the basis of fundamental principles of continuum mechanics of large plastic flow, physical system modeling and irreversible thermodynamics, the Dynamic Materials Model (DMM) was first developed by PRASAD et al[9, 22]. DMM is viewed as a bridge between the continuum mechanics of large plastic deformation and the development of dissipative microstructures in the materials. It can illuminate how the external energy dissipated through the plastic deformation of work piece. The processing map was usually developed using DMM, with the complementary relationship between the rate of visco-plastic heat generation induced by deformation and the rate of energy dissipation associated with microstructural mechanisms occurring during the deformation process. A non-dimensional efficiency index η is used to represent the power dissipation through microstructural mechanisms and is given as follows:

$$\eta = \frac{2m}{m+1} \quad (1)$$

where m is strain rate sensitivity. The variation of η indicates the microstructural changes during hot deformation. The dissipation map can be obtained with the contour plot of η values on the deformation temperature and strain rate field. ZIEGLER[23] proposed the principles of maximum rate of entropy production, from which a condition for microstructural instability is obtained:

$$\xi(\dot{\epsilon}) = \frac{\partial \ln[m/(m+1)]}{\partial \ln \dot{\epsilon}} + m < 0 \quad (2)$$

The parameter $\xi(\dot{\epsilon})$ may be evaluated as a function of temperature and strain rate to obtain an instability map, where metallurgical instabilities during plastic flow are predicted to occur in regimes where $\xi(\dot{\epsilon})$ is negative. The instability map is superimposed on the dissipation map to obtain a processing map. With the help of the processing map, the safe domains and flow instable domains can be determined. The temperature and strain rate corresponding to the peak efficiency in safe domain can be chosen as the optimum parameters for hot working.

4 Artificial neural network modeling

Artificial neural network (ANN), which is

considered artificial intelligence modeling technique, is an intelligent information treatment system with the characteristics of adaptive learning and treating complex and non-linear relationships. It is essentially a “black box” operation linking input to output data using a particular set of nonlinear basis functions. With the development of technology of artificial intelligence, the ANN has become a powerful tool in the simulation and control of various processes.

A general schematic of ANN model for the present investigation is shown in Fig.1. It can be seen from Fig.1 that each neural network consists of an input layer, an output layer and one or more hidden layers. The input layer is used to receive data from outside, while the output layer sends the information out to users. The role of the hidden layer, which is a layer that contains a systematically determined number of processing elements, is to provide the necessary complexity for non-linear problems. The number of units in input and output layers is dictated by the problem, but the number of hidden units which controls the complexity of the model must be determined. Because the sigmoid functions are easily differentiable, the processing units for computational convenience are employed in the present model:

$$f(x) = \frac{1}{1 + \exp(-x)} \quad (3)$$

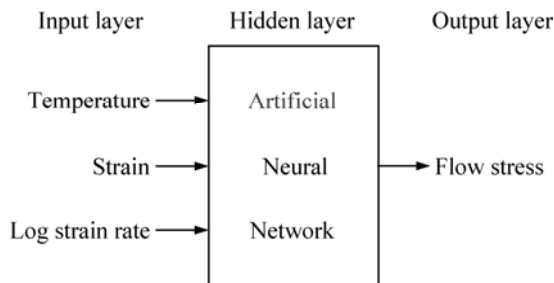


Fig.1 Schematic of ANN model of Ti40 alloy

Based on the hot compression test of Ti40 alloy, the flow stress—strain curves were obtained from the load—displacement data automatically. Fig.2 shows the typical stress—strain curves at different deformation temperatures. In order to develop an ANN model, all the data sets obtained from these curves were divided into two sets. One is to be used to train the network, and the remaining is to be used to verify the generalization capability of the network. A typical neuron receives input signals, sums them according to their weight, passes it through a function and produces an output. This output is then compared with the experimentally obtained outputs, and the error is calculated. This error is then propagated backwards and used for adjusting the weight of each of the neurons. The process of using the

experimental outputs to minimize the mean squared error iteratively is called as training the network. Once the architecture of network is defined, then through learning process, weights are calculated so as to present the desired output, and can be used later for predicting outputs given a different set of inputs.

In this study, because multilayer network has greater representational power to deal with highly non-linear and multivariable system, a multilayer perceptron (MLP)-based feed-forward network trained by back propagation (BP) type learning algorithm was used[24]. Although multilayer neural network does not ensure a global minimum solution for any given problem, it is a reasonable approximation that if the network is trained with a comprehensive database, the resulting model will approximate all of the laws of mechanics that the actual material or process obeys. In the present ANN model, the inputs of the model are strain (ϵ), logarithm strain rate ($\lg \dot{\epsilon}$) and deformation temperature (T). The output of the model is flow stress (σ). Instead of strain rate, logarithm strain rate was chosen because flow stress usually varies with logarithm strain rate on a physical basis.

The input and output parameters must be standardized and fall in the closed interval $[0, 1]$. Because of this conversion method, the normalization technique is used in the proposed ANN according to the following formula:

$$Z' = \frac{Z - 0.95Z_{\min}}{1.05Z_{\max} - 0.95Z_{\min}} \quad (4)$$

where Z is the experimental value of strain, logarithm strain rate, deformation temperature or flow stress; and Z' is the normalized value of Z , which has a maximum and minimum values given by Z_{\min} and Z_{\max} , respectively. Once the best-trained network is found, all the transformed data converts to its equivalent values, which can be expressed as follows:

$$Z = Z'(1.05Z_{\max} - 0.95Z_{\min}) + 0.95Z_{\min} \quad (5)$$

The total experimental data sets were then divided into two parts. Data sets at the strain of 0.4 were removed and the remaining data sets were used for training. The removed datasets were subsequently used for testing the network. A logistic sigmoid function expressed as Eq. (3) was employed as the activation function; the learning is based on gradient descent algorithm and hence requires the activation function to be differentiable. The number of hidden neurons determines the complexity of neural network and precision of predicted values. In this application, 8–15 hidden-layer neurons were employed to test. The algorithm with 12 hidden-layer neurons was suggested to be used in present application since minimum mean

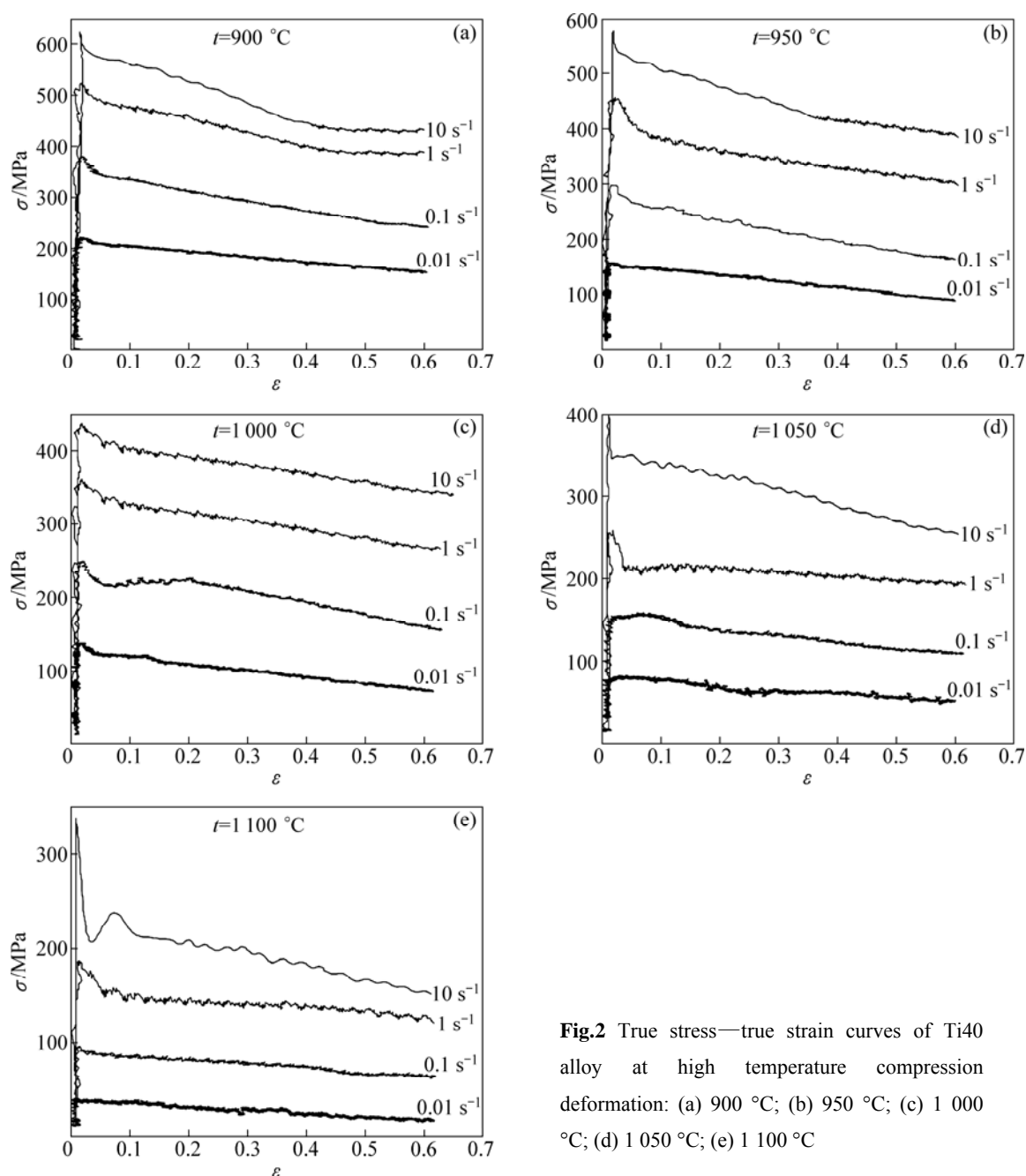


Fig.2 True stress—true strain curves of Ti40 alloy at high temperature compression deformation: (a) 900 °C; (b) 950 °C; (c) 1 000 °C; (d) 1 050 °C; (e) 1 100 °C

square error is obtained. The other parameters of MLP architecture and training are listed in Table 1.

Table 1 Setting of training parameters for neural network

Name of network parameter	Content
Learning algorithm	Back propagation
Training function	Trainlm
Activation functions for hidden and output layers	Log-sigmoid
Performance function	MSE
Training epoch	20 000
Goal	0.000 1

5 Results and discussion

After training the network successfully, it has been tested by using the known training data. Statistical methods are used to compare the results produced by the network. A wide variety of standard statistical performance evaluation measures have been employed to evaluate the model performance. The generalization capability of the training and testing network is quantified in terms of correlation coefficient (R), average absolute relative error (e_{AARE}), average root mean square error (e_{RMSE}) and scatter index (I_S). They are defined as follows, respectively.

$$R = \frac{\sum_{i=1}^N (E_i - \bar{E})(P_i - \bar{P})}{\left(\sum_{i=1}^N (E_i - \bar{E})^2 \sum_{i=1}^N (P_i - \bar{P})^2 \right)^{1/2}} \quad (6)$$

$$e_{\text{AARE}} = \frac{1}{N} \sum_{i=1}^N \left| \frac{E_i - P_i}{E_i} \right| \times 100\% \quad (7)$$

$$e_{\text{RMSE}} = \left[\frac{1}{N} \sum_{i=1}^N (E_i - P_i)^2 \right]^{1/2} \quad (8)$$

$$I_S = \frac{e_{\text{RMSE}}}{\bar{E}} \quad (9)$$

where E is the experimental value and P is the predicted value obtained from the neural network model; \bar{E} and \bar{P} are the mean values of E and P , respectively; N is the total number of data employed in the investigation.

The performance of BP neural network prediction for both the training and testing data is depicted in Table 2. e_{AARE} and e_{RMSE} are computed by comparison of the relative error and therefore are unbiased statistics for measuring the predictability of a model. As can be seen from Table 2, the values of e_{AARE} for the training and test dataset are only 2.890% and 1.814%, respectively, which shows that the generalization capability of the training and testing network is satisfied.

Table 2 Performance of ANN model for training and testing datasets of Ti40 alloy

Dataset	R	$e_{\text{RMSE}}/\%$	$e_{\text{AARE}}/\%$	I_S
Training	0.9982	7.802	2.890	0.034
Testing	0.9992	4.616	1.814	0.021

In addition, the comparison between the experimental and corresponding predicted results for both training and testing datasets of Ti40 alloy is shown in Fig.3. The correlation coefficient is a commonly used statistic and provides information on the strength of linear relationship between observed and computed values. In Fig.3(a), the corresponding correlation coefficient (R) is found to be 0.998 2 which indicates that a very good correlation between experimental and predicted results has been obtained, and suggests that the trained neural network is able to predict the compressive deformation behaviors of Ti40 alloy successfully. Performance of the model for flow stress prediction is shown in Fig.3(b). The correlation coefficient of the testing network is higher than that of training network, indicating that the model prediction fits well with the experimental observation. Therefore, the artificial neural network trained with back propagation algorithm has been developed to present the excellent performance of

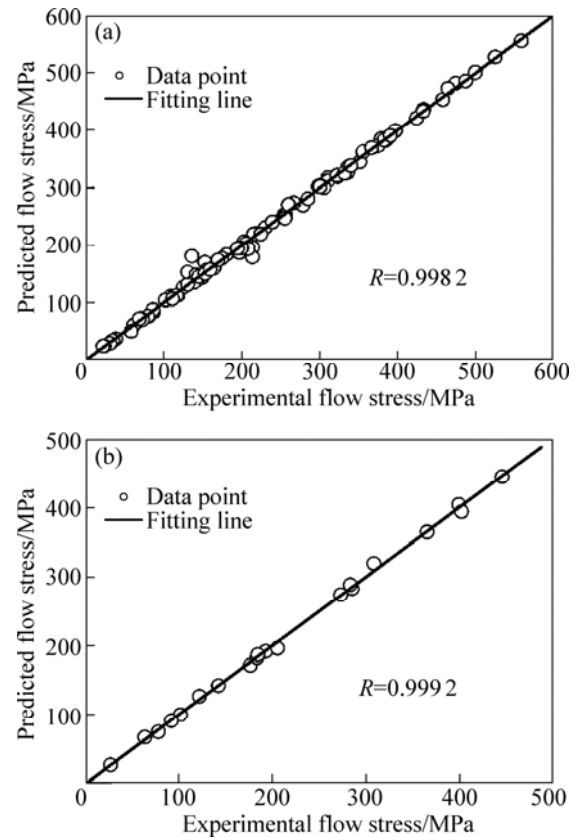


Fig.3 Comparison of flow stress values predicted by BP neural network and experimental values for training (a) and testing dataset (b)

flow stress prediction of Ti40 alloy.

The performance of the ANN model trained with BP algorithm is further investigated by analysis of the absolute relative error of neural network predictions for testing data at strain of 0.4. The results are presented graphically as error bars (Fig.4). It can be found that all the relative errors between predicted and experimental values are within 5%, which suggests that the satisfactory predicted results of ANN model can be used

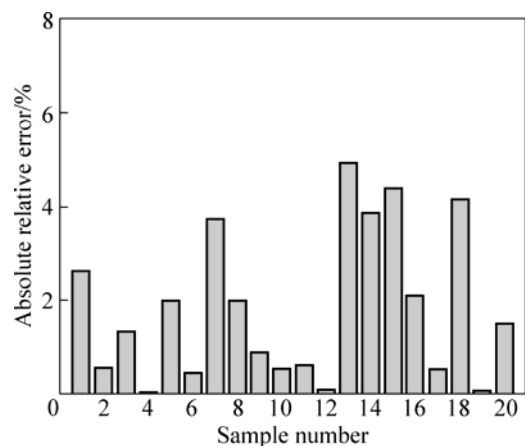


Fig.4 Absolute relative error of neural network predictions compared with experimental values using testing data ($\varepsilon=0.4$)

rather than measured and hence reduce testing time and cost.

Fig.5 shows the processing map drawn according to the predicted results at strain of 0.4 using trained ANN model. The processing map is superimposed by the instability map on the power dissipation map, the contour numbers represent percentage efficiency of power dissipation and shaded region shows the instability region. It is similar to that reported in Ref.[25]. From Fig.5, the map indicates the variation of the efficiency as a function of temperature and log strain rate. At a relatively low temperature (below 950 °C) and high strain rate (above 3 s⁻¹) regime, the dissipation efficiency is less than 15%. However, one domain appears in the temperature range of 990–1 100 °C and at a strain rate lower than 0.01 s⁻¹, with a power efficiency of 60% (at 1 100 °C and 0.01 s⁻¹). The domain appears to extend to lower strain rates and may reach an even higher efficiency. These features suggest that some microstructural changes may happen during the deformation. The contours in the stable domain are generally widely spaced, thus the power dissipation map may provide an initial suggestion of the domain area of dynamic recrystallization. Microstructure analysis reveals that the initial microstructures have been replaced by recrystallized structure (Fig.6). Because dynamic recrystallization (DRX) not only gives good intrinsic workability by simultaneous softening, but also optimizes the microstructure, so the domain corresponds to the optimum hot working conditions. Hence, the optimum processing conditions are in the strain rate range of 0.01–0.05 s⁻¹ and temperature range of 975–1 100 °C, where the efficiencies are much higher compared with other stable region. The material exhibits flow instabilities at strain rates higher than 3 s⁻¹ and in the temperature range of 900–1 000 °C. Microstructural examination of the specimens deformed at 950 °C and the strain rate of 10 s⁻¹ is shown in Fig.7.

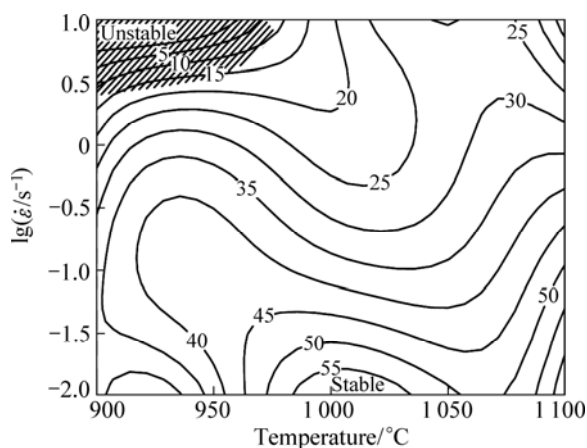


Fig.5 Processing map obtained by ANN model for Ti40 alloy ($\varepsilon=0.4$)

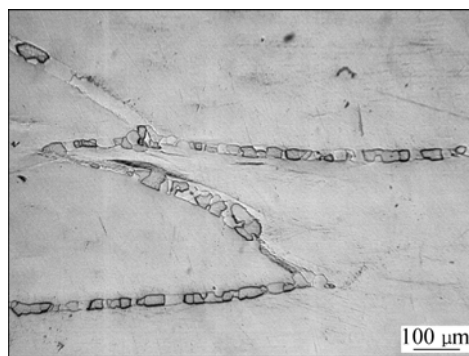


Fig.6 Dynamic recrystallization observed at 1 000 °C and 1 s⁻¹



Fig.7 Microstructure obtained on Ti40 alloy specimens deformed in instability regime showing manifestations in form of shear bands on deformation at 950 °C and 10 s⁻¹

The microstructures exhibit adiabatic shear bands oriented at about 45° with respect to the compression axis. The flow localization is due to the adiabatic shear band present in the metal matrix. Therefore, the instability regime has to be avoided during processing Ti40 alloy.

6 Conclusions

1) Artificial neural network (ANN) modeling has been successfully employed in the present work to model the flow stress of Ti40 alloy as an implicit function of strain, lg strain rate and deformation temperature. The multilayer perceptron (MLP) architecture with back-propagation algorithm was utilized and the network with 12 hidden-layer neurons is suggested to be used in present application as minimum mean square error was obtained. The performance of the neural network model is found to be better as the flow stress can be predicted within an accuracy of ±5%.

2) Based on the theory of Dynamic Materials Model (DMM) and the flow stress predicted by the trained network, a processing map was generated at a strain of 0.4 for Ti40 alloy. The domain at about 1 100 °C and 0.01 s⁻¹ with a peak efficiency of 60% can be considered the optimum domain for hot working, while the domain

in 900–1 000 °C and 3–10 s⁻¹ is unsuitable for hot working operation, and the process conditions must be avoided during the processing of Ti40 alloy.

References

- [1] EZUGWU E O, WANG Z M, Titanium alloys and their machinability-a review [J]. J Mater Process Technol, 1997, 68: 262–274.
- [2] BERCZIK D M. Age hardenable beta titanium alloy: US, 5176762 [P]. 1993–01–29.
- [3] ZHAO Y Q, XIN S W, ZENG W D. Effect of major alloying elements on microstructure and mechanical properties of a highly β stabilized titanium alloy [J]. J Alloys Compd, 2009, 481: 190–194.
- [4] XIN S W, ZHAO Y Q, ZENG W D, WU H. Research on thermal stability of Ti40 alloy at 550 °C [J]. Mater Sci Eng A, 2008, 477: 372–378.
- [5] ZHAO Y Q, ZHOU L, DENG J. The role of interface in the burning of titanium alloys [J]. Mater Sci Eng A, 1999, 267: 163–167.
- [6] ZENG W D, SHU Y, ZHANG X M, ZHOU Y G, ZHAO Y Q, WU H, DAI Y, YANG J, ZHOU L. Hot workability and microstructure evolution of highly β stabilised Ti-25V-15Cr-0.3Si alloy [J]. Mater Sci Technol, 2008, 24: 1222–1229.
- [7] ZHANG Xue-min, ZENG Wei-dong, SHU Ying, ZHOU Yi-gang, ZHAO Yong-qing, WU Huan, YU Han-qing. Fracture criterion for predicting surface cracking of Ti40 alloy in hot forming processes [J]. Trans Nonferrous Met Soc China, 2009, 19(2): 267–271.
- [8] ZHAO Y Q, QU H L, ZHU K Y, WU H, LIU C L, ZHOU L. The second phases in Ti40 burn resistant alloy after high temperature exposure for a long time [J]. J Alloys Compd, 2002, 333: 165–169.
- [9] PRASAD Y V R K, GEGAL H L, DORAIVELU S M, MALAS J C, MORGAN J T, LARK K A. Modeling of dynamic material behavior in hot deformation: Forging of Ti-6242 [J]. Metall Trans A, 1984, 15: 1883–1892.
- [10] GRONOSTAJSKI Z. The deformation processing map for control of microstructure in CuAl9.2Fe3 aluminium bronze [J]. J Mater Process Technol, 2002, 125–126: 119–124.
- [11] TAN S P, WANG Z H, CHENG S C, LIU Z D, HAN J C, FU W T. Processing maps and hot workability of Super304H austenitic heat-resistant stainless steel [J]. Mater Sci Eng A, 2009, 517: 312–315.
- [12] CAI D Y, XIONG L Y, LIU W C, SUN G D, YAO M. Characterization of hot deformation behavior of a Ni-base superalloy using processing map [J]. Mater Des, 2009, 30: 921–925.
- [13] BALASUBRAHMANYAM V V, PRASAD Y V R K. Hot deformation mechanisms in metastable beta titanium alloy Ti-10V-2Fe-3Al [J]. Mater Sci Technol, 2001, 17: 1222–1228.
- [14] PHANIRAJ M P, LAHIRI A K. The applicability of neural network model to predict flow stress for carbon steels [J]. J Mater Process Technol, 2003, 141: 219–227.
- [15] MANDAL S, SIVAPRASAD P V, VENUGOPAL S, MURTHY K P N. Artificial neural network modeling to evaluate and predict the deformation behavior of stainless steel type AISI 304L during hot torsion [J]. Appl Soft Comput, 2009, 9: 237–244.
- [16] KAPOOR R, PAL D, CHAKRAVARTTY J K. Use of artificial neural networks to predict the deformation behavior of Zr-2.5Nb-0.5Cu [J]. J Mater Process Technol, 2005, 169: 199–205.
- [17] LIU J T, CHANG H B, HSU T Y, RUAN X Y. Prediction of the flow stress of high-speed steel during hot deformation using a BP artificial neural network [J]. J Mater Process Technol, 2000, 103: 200–205.
- [18] MANDAL S, SIVAPRASAD P V, VENUGOPAL S, MURTHY K P N, RAJ B. Artificial neural network modeling of composition-process-property correlations in austenitic stainless steels [J]. Mater Sci Eng A, 2008, 485: 571–580.
- [19] MALINOV S, SHA W, MCKEOWN J J. Modelling the correlation between processing parameters and properties in titanium alloys using artificial neural network [J]. Comput Mater Sci, 2001, 21: 375–394.
- [20] SHA W, EDWARDS K L. The use of artificial neural networks in materials science based research [J]. Mater Des, 2007, 28: 1747–1752.
- [21] BHADESHIA H K D H, DIMITRIUL R C, FORSIKL S, PAK J H, RYU J H. Performance of neural networks in materials science [J]. Mater Sci Technol, 2009, 25: 504–510.
- [22] PRASAD Y V R K. Recent advances in the science of mechanical processing [J]. Indian J Tech, 1990, 28: 435–451.
- [23] ZIEGLER H. Progress solid mechanism [M]. New York: Wiley, 1963: 63–193.
- [24] JUANG S C, TARNG Y S, LII H R. A comparison between the back-propagation and counter-propagation networks in the modeling of the TIG welding process [J]. J Mater Process Technol, 1998, 75: 54–62.
- [25] ZENG Wei-dong, ZHOU Yi-gang, SHU Ying, ZHAO Yong-qing, YANG Jin, ZHANG Xue-min. A study of hot deformation mechanisms in Ti-40 burn resistant titanium alloy using processing maps [J]. Rare Metal Materials and Engineering, 2007, 36(1): 1–6. (in Chinese)

应用人工神经网络构造 Ti40 合金加工图

孙 宇¹, 曾卫东¹, 赵永庆², 张学敏¹, 马 雄¹, 韩远飞¹

1. 西北工业大学材料学院 凝固技术国家重点实验室, 西安 710072;

2. 西北有色金属研究院, 西安 710016

摘 要: 以 Gleeble-1500 热模拟试验机获得的 Ti40 钛合金压缩试验数据为基础, 应用人工神经网络对数据进行训练和预测, 建立该合金的高温流动应力与应变、应变速率和温度对应关系的预测模型, 其中, 应变、应变速率 (对数形式) 和变形温度作为模型的输入参数, 流动应力作为模型的输出参数。结果发现, 运用 BP 反向传播算法进行训练的神经网络模型具有良好的预测功能, 其预测值与实验测量值基本吻合。同时, 采用神经网络模型预测的数据构造 Ti40 合金的加工图, 其安全区和失稳区的范围与实测数据获得的加工图基本相符, 并对各自区域的相应组织状态进行金相观察。

关键词: Ti40 合金; 加工图; 人工神经网络

(Edited by YANG Hua)